Mathematical Biosciences and Engineering

http://www.aimspress.com/journal/MBE

MBE, 16(5): 5247–5262.
DOI: 10.3934/mbe.2019262
Received: 07 February 2019
Accepted: 22 May 2019
Published: 10 June 2019

Research article

CSB modulates the competition between HIF-1 and p53 upon hypoxia

Xiao-Wei Ye[1], **Xiao-Peng Zhang**[2,3,*] **and Feng Liu**[1,3,*]

[1] National Laboratory of Solid State Microstructures, Department of Physics, and Collaborative Innovation Center of Advanced Microstructures, Nanjing University, Nanjing 210093, P.R. China

[2] Kuang Yaming Honors School, Nanjing University, Nanjing 210023, P.R. China

[3] Institute for Brain Sciences, Nanjing University, Nanjing 210093, P.R. China

* **Correspondence:** Email: zhangxp@nju.edu.cn, fliu@nju.edu.cn.

Abstract: Both hypoxia-inducible factor-1 (HIF-1) and tumor suppressor p53 are involved in the cellular response to hypoxia. It has been reported that HIF-1α induces cockayne syndrome B (CSB) to compete with p53 for limited p300. We developed a network model to clarify how the interplay between HIF-1 and p53 modulates cellular output in the presence of CSB. Our results revealed that HIF-1α is progressively activated depending on the severity of hypoxia. Activated HIF-1α promotes its own activation by inducing CSB to dissociate p300 from p53 under moderate hypoxia; in severe hypoxia, p53 accumulates remarkably due to ATR-dependent phosphorylation and wins the competition for p300. As a result, HIF-1α induces PFKL and VEGF to facilitate cellular adaptation to mild and moderate hypoxia respectively, while p53 is activated to induce apoptosis under severe hypoxia. This work may advance the understanding of the modulation of the interplay between HIF-1 and p53 in the hypoxic response.

Keywords: network model; HIF-1α; p53; CSB; hypoxia

1. Introduction

Hypoxia induced factor 1 (HIF-1) plays a key role in cellular response to hypoxia [1]. It is a heterodimer composed of an oxygen-sensitive HIF-1α subunit and a constitutively expressed HIF-1β subunit [2]. Under normoxia, HIF-1α is hydroxylated at Pro402 and Pro564 in the N-terminal transactivation domain (N-TAD) by prolyl hydroxylase domain proteins (PHDs) that facilitate HIF-1α degradation by von Hippel-Lindau (VHL) [2,3]; HIF-1α is deactivated due to hydroxylation at Asn803 in the C-terminal transactivation domain (C-TAD) by factor inhibiting HIF-1 (FIH) that blocks its interaction with the co-activator p300/CBP [4]. Upon hypoxia, HIF-1α accumulates remarkably and is activated due to the gradual deactivation of PHD and FIH [5]. Active HIF-1α induces a large number

of genes involved in cellular adaptation to hypoxia [1]. It is less understood how the two transactivation domains of HIF-1α coordinate in cell fate decision.

p53 is a well-known tumor suppressor involved in cellular response to multiple stresses including DNA damage [6–8]. It is also activated and plays a significant role in response to hypoxia [9]. It has been reported that HIF-1α induces cockayne syndrome B (CSB) to inhibit p53 activation [10]. HIF-1α and p53 compete for limited p300 for transactivation [11]. Binding of CSB to p53 disassociates it from p300 and promotes HIF-1α activation indirectly, enclosing a positive feedback loop [12]. CSB deficiency leads to cellular fragility, while overexpressed CSB increases the risk of cell carcinogenesis [13]. It is intriguing to clarify how CSB modulates the competition between HIF-1α and p53.

The mechanism of p53 stabilization upon hypoxia is rather complicated. For example, HIF-1α promotes the stabilization of wild-type p53 in cells treated with hypoxia mimics [14]. Direct interaction between HIF-1α and Mdm2 protects p53 from degradation [15]. Moreover, ataxia-telangiectasia and Rad3-related (ATR) is activated by replication arrest under severe hypoxia, and phosphorylates p53 at Ser15 to block Mdm2-dependent degradation, resulting in marked accumulation of p53 [16]. Protein phosphatase-1 nuclear targeting subunit (PNUTS) is induced to repress p53 dephosphorylation via protein phosphatase-1, promoting p53 accumulation indirectly [17]. Once p53 reaches high levels and is acetylated by p300, apoptosis is induced [18]. An issue arises concerning how p53 is activated in the presence of CSB expression.

A series of models have been developed to investigate how the HIF-1 network responds to hypoxia [19]. Qutub *et al.* proposed a detailed model of oxygen sensing by HIF-1α to clarify the mechanism underlying its dynamic behaviors [20]. Nguyen *et al.* focused on the progressive activation of HIF-1α by sequential deactivation of PHD and FIH under gradually aggravating hypoxia [21]. Bagnal *et al.* characterized the role of the HIF-1-PHD negative feedback loop in the pulsing behavior of HIF-1α [22]. Recently, we built a network model to characterize the competition between HIF-1α and p53 for p300, focusing on the mechanism underlying the regulation of HIF-1α activity and apoptosis induction by p53 [9]. It is still a challenge to explore the mechanism for interplay between the two pathways in response to hypoxia.

In this work, we developed a network model to unravel how CSB modulates the competition between HIF-1α and p53 in their activation upon hypoxia. We revealed that HIF-1α and p53 induce CSB and Mdm2 respectively to regulate their activities and influence cellular outcome. Under mild or moderate hypoxia, HIF-1α induces CSB to prevent p53 from activation by p300. Under severe hypoxia, p53 accumulates markedly due to ATR-dependent phosphorylation and prevails over HIF-1α. Abundant p53 competes with HIF-1α for p300, leading to downregulation of CSB and promoting further activation of p53. Together, HIF-1α and p53 can be activated sequentially due to the alternation in the predominance of antagonistic feedback loops.

2. Materials and method

2.1. Model

We built a network model to investigate the interplay between HIF-1α and p53 upon hypoxia. The model characterizes their activation and clarifies the mechanism of cell fate decision (Figure 1). The network model is composed of HIF-1 module, p53 module and the downstream effector module. The HIF-1α and p53 modules are interlinked by p300, CSB and Mdm2. Three feedback loops, i.e., HIF-

1α-CSB-p53, p53-Mdm2 and p53-Mdm2-HIF-1α loops, play significant roles in the hypoxic response. The products of the target genes phosphofructokinase L (PFKL), vascular endothelial growth factor (VEGF) and PUMA act as effectors to decide the cellular outcome. All the regulation relationships in the network are characterized by ordinary differential equations (ODEs) in Method S1 in Supporting Information. The details of the model are presented as follows.

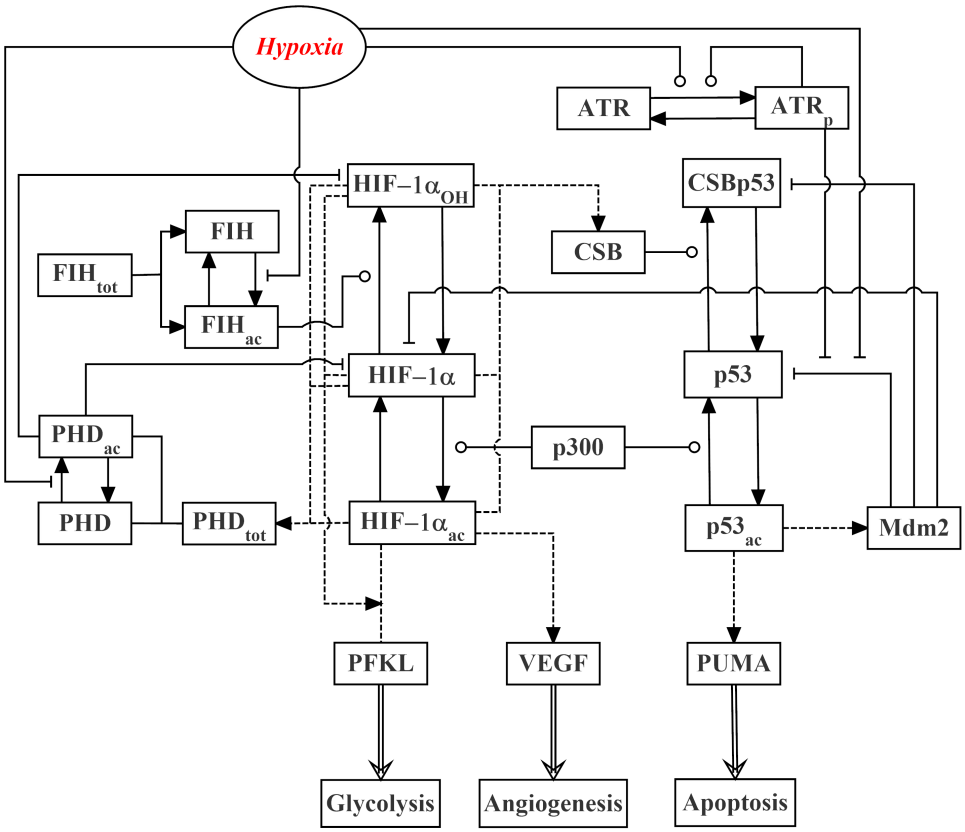

Figure 1. Schematic diagram of the network model involving p53 and HIF-1 pathways in the hypoxic response. The model characterizes the regulation of HIF-1α and p53. CSB modulates the competition between HIF-1α and p53 for p300, influencing the induction of their target genes including PFKL, VEGF and PUMA. The process of transactivation is described by arrow-headed dashed lines, while translation and transition are denoted by arrow-headed solid lines. Circle-headed lines denote promotion, while bar-headed lines indicate repression in enzymatic reactions.

2.2. Regulation of HIF-1α by oxygen levels

HIF-1α is mainly regulated by the hydroxylases PHD (mainly corresponding to PHD-2 in our model) and FIH whose hydroxylation activity is dependent on oxygen levels [2]. The two hydroxylases are deactivated under different hypoxic conditions [23]. In our model, two forms of PHD are considered: PHD (inactive form) and PHD_{ac} (active form); Similarly, FIH is divided into FIH (inactive form) and FIH_{ac} (active form) [21]. According to experimental observation [23], we assume that the dissociation constant of PHD for oxygen is much greater than that of FIH

(Eqns 9,10). Active PHD promotes HIF-1α degradation, while activated FIH represses the C-TAD transcriptional activity of HIF-1α (Eqns 5-6). The total level of PHD, PHD_{tot}, is controlled by HIF-1 since the PHD-2 gene is considered an N-TAD gene [5]. The total level of FIH is assumed to be constant and is denoted by FIH_{tot} (Eqn 2) .

Based on its modification status, three forms of HIF-1α are considered: HIF-1α (dehydroxylated form), HIF-1α_{OH} (C-TAD hydroxylated form) and HIF-1α_{ac} (C-TAD acetylated form). Dehydroxylated HIF-1α can transform into HIF-1α_{OH} through FIH-induced hydroxylation in C-TAD. Under mild hypoxia, the deactivation of PHD promotes the stabilization of HIF-1α. HIF-1α_{OH} has partial transcriptional activity because of its N-TAD activity (Eqn 6) [5]. Under moderate hypoxia, acetylated HIF-1α accumulates due to further deactivation of FIH [24]. HIF-1α is fully activated into HIF-1α_{ac} by recruiting p300 (Eqn 7) [4, 25]. The conversion between different forms of HIF-1α is characterized by the Michaelis-Menten kinetics.

We assume that all the three forms of HIF-1α can transactivate the N-TAD-inducible genes like PHD, CSB and PFKL [5, 10]. PHD production is controlled by each form of HIF-1α (Eqn 8) [26]. Given that CSB disassociates p300 from p53, we assume that HIF-1α induces CSB to form the CSBp53 complex, preventing p53 from activation by p300 (Eqns 13-14) [12]. Thus, HIF-1α promotes its own activation in a positive feedback loop [12]. PFKL is modulated by N-TAD of HIF-1α, inducing glycolysis [5, 27]. For simplicity, the rate constants for the transactivation of each N-CAD-inducible gene by the three forms of HIF-1α are set to the same values. In addition, it is assumed that VEGF is a C-TAD-inducible gene, and can only be activated by HIF-1α_{ac} [5, 28]. All the induction rates of those target genes are described by Hill functions.

2.3. p53 regulation upon hypoxia

Hypoxia contributes to p53 stabilization by the ATR-dependent and -independent mechanisms that repress Mdm2-dependent degradation (Eqn 11) [17]. On one hand, ATR is activated in severe hypoxia [16], and activated ATR promotes its further phosphorylation, enclosing a positive feedback loop (Eqn 16) [29]. Given posttranslational modification is the main mode of ATR regulation [30], the total level of ATR, ATR_{tot}, is assumed to be a constant. Since hypoxia promotes the phosphorylation of ATR, we assumed that the activation rate of ATR is a decreasing function of oxygen levels. On the other hand, given the effect of PNUTS on p53 stabilization, it is assumed that p53 degradation rate is an increasing function of oxygen levels (Eqn 11) [15, 26].

Three forms of p53 are considered: p53 (free inactive form), $p53_{ac}$ (acetylated form) and CSBp53 (p53 in complex with CSB). Once p53 is stabilized, it competes with HIF-1α for p300 [11]. It is assumed that p53 has a higher affinity for p300 than HIF-1α [12]. Interestingly, the transcriptional activity of primarily accumulated p53 is repressed by CSB through forming the CSBp53 complex and excluding the binding of p300 [12]. p53 can be acetylated into $p53_{ac}$ by p300, which has transcriptional activity and induces target genes. $p53_{ac}$ induces Mdm2 to promote the degradation of both HIF-1α and p53 [31]. As a result, p53 promotes its own degradation by inducing Mdm2 in a negative feedback loop, and indirectly facilitate its own activation by inducing Mdm2 to degrade its competitor HIF-1α in a positive feedback loop. We assume that free p53, CSBp53 and HIF-1α compete for Mdm2 in their degradation [15]. PUMA is induced by p53 to initiate apoptosis [32]. Hill function is exploited to describe the transcription of p53-targeted genes, and the Hill coefficient is set to 4 since p53 is mostly present in tetramers transactivating target genes [33].

2.4. Methods and parameters

The details of the model and parameter setting are presented in Supporting Information. The dynamics of all the species are characterized by ordinary differential equations (ODEs) in Method S1. [.] denotes the concentration of each species. The initial concentration of each species is set to its steady-state value at 21% O_2 (Table S1). All parameter values are listed in Table S2. The software Oscill8 is used to numerically solve the ODEs and plot bifurcation diagrams. In our model, oxygen concentration refers to the percentage of oxygen in volume denoted by L_{O_2}, which corresponds to oxygen concentration in the culture environment in experiments [1]. For culture cells, oxygen concentration can vary from 21% to 0%. Roughly, mild hypoxia refers to oxygen concentration in the range of 1%–5%, moderate hypoxia corresponds to 0.1%–1% O_2, and oxygen concentration is below 0.1% for severe hypoxia [34]. Of note, oxygen concentration in cells is markedly lower than that in the culture systems [34].

3. Results

3.1. Overview of the dynamics of key proteins

Figure 2 shows the dynamics of key proteins in the network under mild, moderate or severe hypoxia. Under mild hypoxia (2% O_2), partially activated HIF-1α_{OH} accumulates markedly due to deactivation of PHD (Figure 2A). HIF-1α_{ac} and p53 remain at rather low levels. PFKL is transactivated by HIF-1α_{OH} and rises to high levels to induce glycolysis. VEGF and PUMA are not induced in this case.

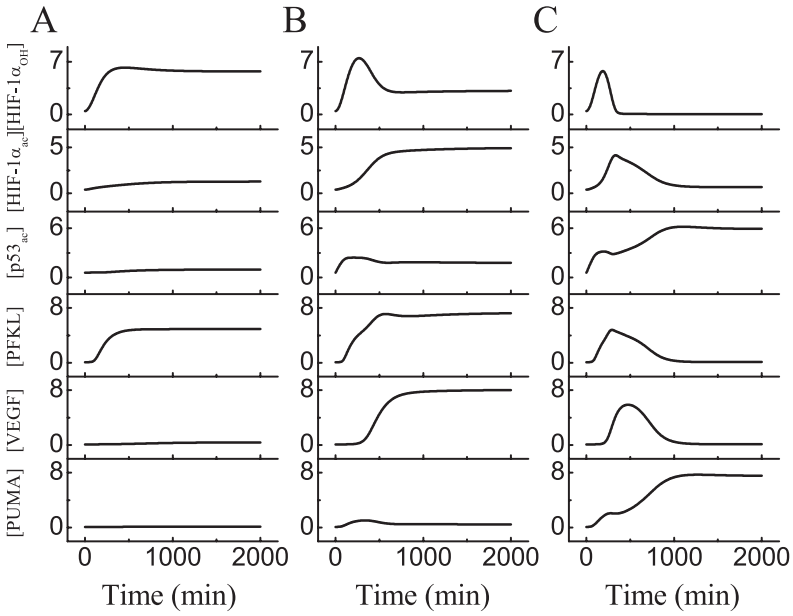

Figure 2. Overview of the network dynamics under different hypoxic conditions. Temporal evolution of the levels of HIF-1α_{OH}, HIF-1α_{ac}, $p53_{ac}$, PFKL, VEGF and PUMA under mild hypoxia (2% O_2) (A), moderate hypoxia (0.4% O_2) (B), or severe hypoxia (0.02% O_2) (C).

For moderate hypoxia (0.4% O_2), HIF-1α_{OH} first accumulates due to hypoxia-induced stabilization and drops significantly due to the deactivation of FIH (Figure 2B). Subsequently, HIF-1α is further acetylated by p300 and activated into fully active HIF-1α_{ac}. As a result, the C-ATD-activated gene VEGF is expressed to promote angiogenesis. PFKL also reaches high levels since it is still induced by HIF-1α_{ac}. A little amount of p53 is activated and the PUMA level rises mildly.

For severe hypoxia (0.02% O_2), both HIF-1α_{OH} and HIF-1α_{ac} rises in the early phase since PHD deactivation leads to HIF-1α stabilization; they drop to basal levels due to Mdm2-dependent degradation since $p53_{ac}$ rises to high levels and promotes Mdm2 production (Figure 2C). The phase difference between p53 and HIF-1α contributes to the adaptive behaviors of HIF-1α. Consequently, [PFKL] and [VEGF] decline to basal levels in the late phase following the fall in [HIF-1α]. $p53_{ac}$ induces PUMA to trigger apoptosis. These results are consistent with the experimental observation that p53 accumulates markedly only in severe hypoxia [16].

The above results suggest that HIF-1 and p53 are antagonistic in the hypoxic response. HIF-1α is progressively activated from mild to moderate hypoxia, while p53 is only activated under severe hypoxia. The cell fate shifts from HIF-1-dependent survival to p53-induced apoptosis. How hypoxia severity modulates the interplay between HIF-1 and p53 will be revealed in the following.

3.2. HIF-1α is progressively activated upon hypoxia

The bifurcation diagrams of [HIF-1α_{OH}] and [HIF-1α_{ac}] versus O_2% are plotted to show the dependency of HIF-1α activation on the severity of hypoxia (Figure 3A). [HIF-1α_{OH}] first rises with decreasing oxygen levels due to enhanced stabilization of HIF-1α that is hydroxylated by FIH. It reaches the peak during the transition region between mild and moderate hypoxia (about at 1.2% O_2) and then decays to basal levels under severe hypoxia. In contrast to HIF-1α_{OH}, HIF-1α_{ac} rises more gradually, reaches the peak at a lower oxygen level under moderate hypoxia (about 0.5% O_2), and drops to basal levels for severe hypoxia. Our results show agreements with experimental observation that the prolyl hydroxylation sites in HIF-1α is sensitive to hypoxia than the asparaginyl hydroxylation sites [24]. Thus, HIF-1α is progressively activated with gradually aggravating hypoxia.

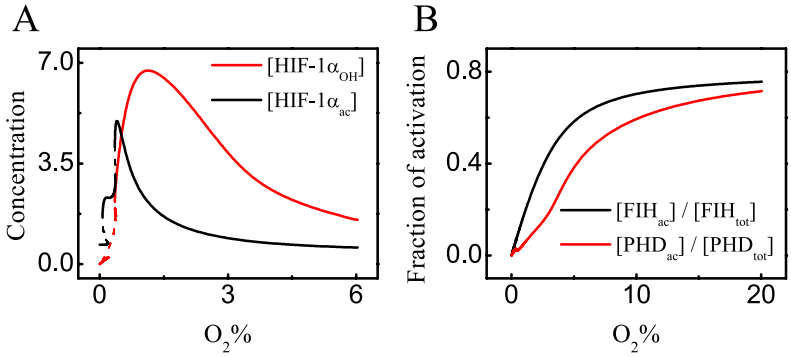

Figure 3. Progressive activation of HIF-1α in response to hypoxia. (A) Bifurcation diagrams of the steady-state levels of HIF-1α_{OH} and HIF-1α_{ac} versus O_2%. (B) Fraction of [PHD_{ac}] and [FIH_{ac}] versus O_2%.

Figure 3B shows the fraction of PHD_{ac} and FIH_{ac} versus $O_2\%$. With decreasing oxygen levels, the fraction of PHD_{ac} reduces gradually under mild hypoxia, while the fraction of FIH_{ac} remains at high levels and declines markedly under moderate or severe hypoxia. The difference in the curves can be explained by their distinct sensitivity to hypoxia. PHD is deactivated earlier than FIH with decreasing oxygen levels, which means PHD is more sensitive to hypoxia than FIH [24]. Deactivation of PHD contributes to the stabilization of HIF-1α, and HIF-1α_{OH} rises under mild hypoxia (see Figure 3A). When oxygen level further drops, HIF-1α_{OH} is further dehydroxylated due to deactivation of FIH, facilitating the accumulation of HIF-1α_{ac} in moderate hypoxia.

3.3. HIF-1α promotes its own activation by inducing CSB

It is assumed that CSB induction is controlled by both HIF-1α_{OH} and HIF-1α_{ac}. We first investigate the significance of HIF-1α_{OH}-dependent CSB induction in activation of HIF-1α_{ac}. The bifurcation diagrams of [HIF-1α_{ac}] versus $O_2\%$ are plotted for different induction rates of CSB by HIF-1α_{OH} (Figure 4A). [HIF-1α_{ac}] drops remarkably in the absence of CSB induction, especially under moderate hypoxia. This variation is relevant to the inhibition of p53 by CSB. With $k_{hifohcsb} = 0$, the level of CSBp53 declines due to reduced CSB expression and p53 snatches p300 from HIF-1α_{ac}, thereby leading to the reduction in [HIF-1α_{ac}] (Figure 4B). Therefore, HIF-1α_{OH} induces CSB to facilitate HIF-1α activation by separating p53 from p300.

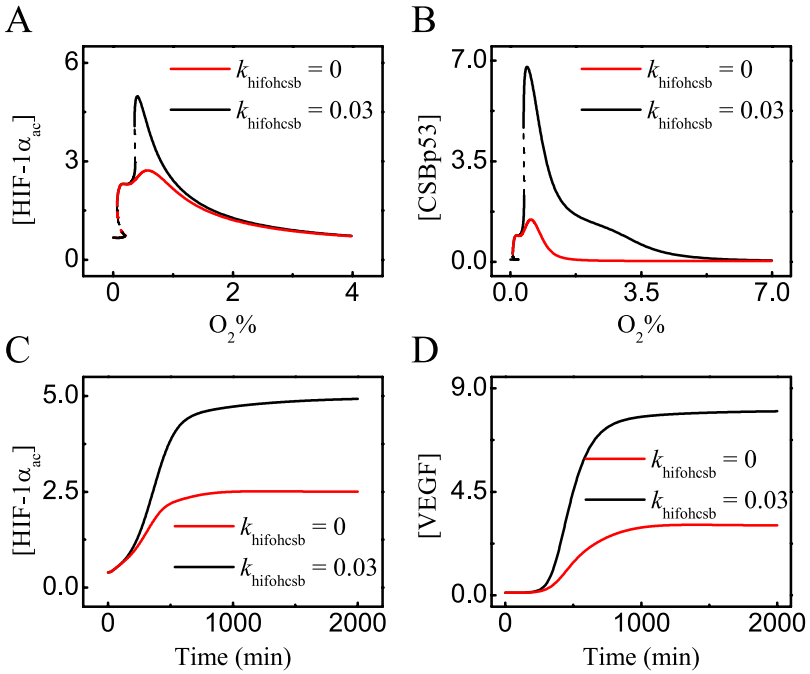

Figure 4. HIF-1α_{OH}-dependent CSB induction facilitates the activation of HIF-1α_{ac}. (A-B) Bifurcation diagrams of [HIF-1α_{ac}] (A) and [CSBp53] (B) versus $O_2\%$ with or without HIF-1α_{OH}-dependent CSB induction. (C, D) Time courses of [HIF-1α_{ac}] (C) and [VEGF] (D) at 0.4% O_2 for different rates of HIF-1α_{OH}-dependent CSB induction.

The dynamics of [HIF-1α_{ac}] are shown under moderate hypoxia (Figure 4C). When $k_{hifohcsb}$ reduces from 0.03 to 0, the steady-state of [HIF-1α_{ac}] declines to a medium level (see Figure 4A). As a result, the steady-state level of VEGF drops significantly without HIF-1α_{OH}-induced CSB expression (Figure 4D).

The significance of HIF-1α_{ac}-CSB-p53 positive feedback in HIF-1α_{ac} activation is further investigated (Figure 5). A global view of HIF-1α_{ac} dynamics under various hypoxic conditions is presented with heat maps. With normal CSB expression, HIF-1α_{ac} is activated persistently only under moderate hypoxia (Figure 5A). Moreover, the initial values of the variables are set to the steady states at 0% O_2 and the above heat map is redrawn (Figure S1A). Compared to Figure 5A, [HIF-1α_{ac}] reaches low steady states in the transition region of severe and moderate hypoxia due to existing bistability in the region (see Figure 3A). With $k_{hifaccsb} = 0$, [HIF-1α_{ac}] only rises to high levels transiently (Figure 5B). Therefore, the HIF-1α_{ac}-CSB-p53 feedback loop is required for sustained activation of HIF-1α.

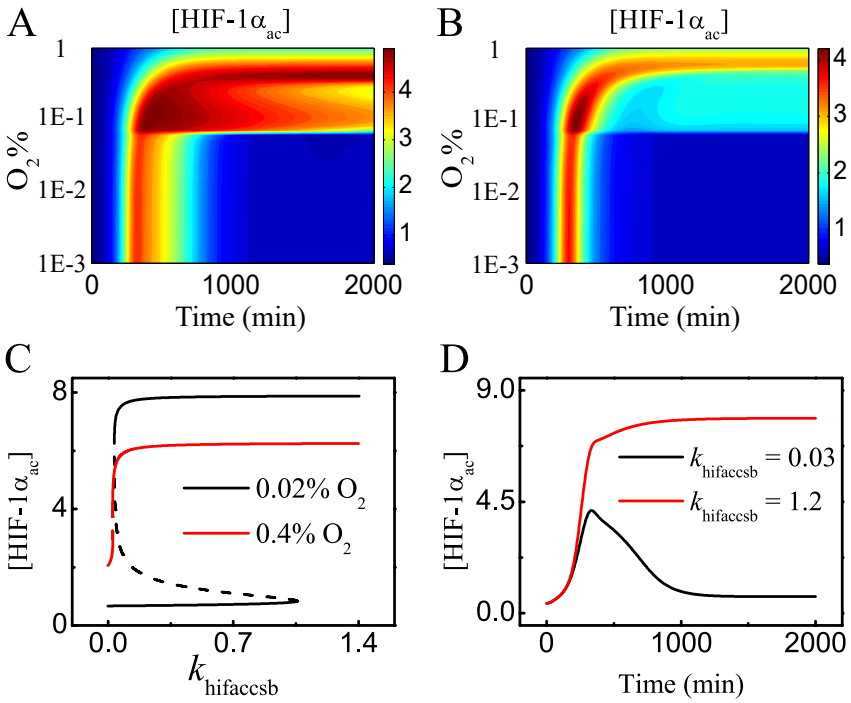

Figure 5. HIF-1α_{ac} induces CSB to promote its own activation. (A, B) Heat maps of [HIF-1α_{ac}] as a function of oxygen concentration and time with $k_{hifaccsb} = 0.03$ (A) or 0 (B). (C) Bifurcation diagram of [HIF-1α_{ac}] versus $k_{hifaccsb}$ at 0.4% or 0.02% O_2. (D) Time courses of [HIF-1α_{ac}] with $k_{hifaccsb} = 0.03$ or 1.2 at 0.02% O_2.

To investigate the influence of $k_{hifaccsb}$ on HIF-1α_{ac} activation, we plot the bifurcation diagrams of [HIF-1α_{ac}] versus $k_{hifaccsb}$ under moderate or severe hypoxia (Figure 5C). For moderate hypoxia, [HIF-1α_{ac}] remains at high levels except for very small $k_{hifaccsb}$. For severe hypoxia (0.02% O_2), [HIF-1α_{ac}] exhibits bistability and switches to high levels only when $k_{hifaccsb}$ is very large. When $k_{hifaccsb}$ is rather large, HIF-1α_{ac} rises to high levels since excessive CSB is in complex with all p53, leading to

high expression of HIF-1α_{ac} (Figure 5D). Thus, overexpression of CSB activates HIF-1α indirectly by inhibiting p53 although p53 accumulates remarkably. These results show agreements with the report that CSB is overexpressed in cancer cells, leading to apoptotic resistance [35].

3.4. Activation of p53 in severe hypoxia

We have shown that HIF-1α is progressively activated under mild and moderate hypoxia, but drops to low levels under severe hypoxia. The dynamics of p53 for various oxygen levels are characterized by the heat map (Figure 6A). Alternatively, we replot the heat map by setting the initial values of the variables to the steady states at 0% O_2 (Figure S1B). p53 shows high steady states upon moderate hypoxia due to the existence of bistability in this region (also see Figure 6D). There exists an apparent threshold of oxygen levels for p53 activation. p53 accumulates mildly in moderate hypoxia, and [$p53_{ac}$] rises and reaches rather high levels finally. Thus, p53 is fully activated under severe hypoxia. The heat map of [CSBp53] is also plotted to show the repression of p53 by CSB (Figure 6B). For moderate hypoxia, most p53 is bound by CSB and the CSBp53 complex shows high levels. For severe hypoxia, the amount of CSBp53 drops to rather low levels, leading to p53 activation. As a result, PUMA is induced by $p53_{ac}$ to trigger apoptosis only under severe hypoxia (Figure 6C).

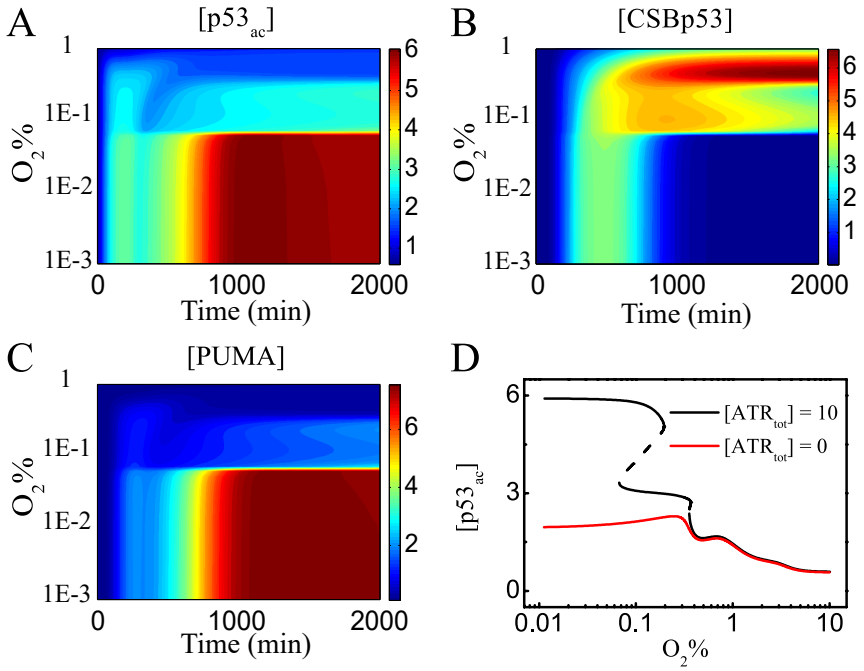

Figure 6. p53 is activated in severe hypoxia. (A-C) Heat maps of [$p53_{ac}$] (A) , [CSBp53] (B) and [PUMA] (C) as a function of O_2% and time. (D) Bifurcation diagrams of [$p53_{ac}$] versus O_2% for different [ATR_{tot}].

It has been reported that ATR promotes p53 stabilization under severe hypoxia [16]. The significance of ATR in p53 activation is assessed by the bifurcation diagrams of [$p53_{ac}$] versus O_2% with or without ATR (Figure 6D). In the normal case, p53 is activated progressively: [$p53_{ac}$] rises to

medium levels in moderate hypoxia and further switches to high levels in severe hypoxia. However, [$p53_{ac}$] only attains medium levels for severe hypoxia in the ATR-deficient case. Therefore, ATR is required for full activation of p53 in response to severe hypoxia.

3.5. Regulation of HIF-1α by the competition between CSB and Mdm2

Once activated, p53 promotes HIF-1α degradation in an oxygen-independent way by inducing Mdm2. Given the indirect repression of p53 by HIF-1α, the p53-Mdm2-HIF-1α positive feedback loop is enclosed. On the other hand, HIF-1α induces CSB to repress p53, enclosing the HIF-1α-CSB-p53 positive feedback loop. The effect of the competition between the two feedback loops on HIF-1α regulation is investigated as follows.

To show the effect of p53-dependent Mdm2 induction on HIF-1α activation, the bifurcation diagrams of [HIF-$1\alpha_{ac}$] versus the induction rate of Mdm2 by p53, $k_{p53mdm2}$, are plotted with $k_{hifohcsb}$ = 0.03 or 0.015 at 0.4% O_2 (Figure 7A). [HIF-$1\alpha_{ac}$] declines with increasing $k_{p53mdm2}$ due to Mdm2-dependent degradation of HIF-1α. For larger $k_{hifohcsb}$, [HIF-$1\alpha_{ac}$] exhibits bistability with varying $k_{p53mdm2}$. [HIF-$1\alpha_{ac}$] drops to low levels only when $k_{p53mdm2}$ exceeds the threshold. For smaller $k_{hifohcsb}$, [HIF-$1\alpha_{ac}$] becomes monostable and drops to low levels more quickly. Therefore, HIF-$1\alpha_{OH}$-dependent CSB induction significantly affects the deactivation of HIF-$1\alpha_{ac}$ by p53-induced Mdm2. The dynamics of HIF-$1\alpha_{ac}$ are shown for different $k_{p53mdm2}$ (Figure 7B). [HIF-$1\alpha_{ac}$] rises to and stays at high levels for smaller $k_{p53mdm2}$, whereas [HIF-$1\alpha_{ac}$] shows a transient pulse for larger $k_{p53mdm2}$ since HIF-1α is activated before marked accumulation of Mdm2 and drops due to degradation by Mdm2.

We have shown that HIF-$1\alpha_{ac}$ promotes its own activation by inducing CSB (see Figure 5). We further plot the bifurcation diagrams of [HIF-$1\alpha_{ac}$] versus $k_{hifaccsb}$ for different $k_{p53mdm2}$ at 0.02% O_2 (Figure 7C). [HIF-$1\alpha_{ac}$] exhibits bistability with varying $k_{hifaccsb}$. With increasing $k_{p53mdm2}$, the threshold for HIF-$1\alpha_{ac}$ activation moves rightward, meaning that more CSB is needed to ensure high expression of HIF-$1\alpha_{ac}$. When $k_{p53mdm2}$ exceeds the threshold, [HIF-1α] always stays at low levels since the p53-Mdm2-HIF-1α loop prevails over the HIF-1α-CSB-p53 loop. The time courses of [HIF-$1\alpha_{ac}$] are shown in Figure 7D. $k_{p53mdm2}$ influences the adaptive behaviors of HIF-$1\alpha_{ac}$ under severe hypoxia. [HIF-$1\alpha_{ac}$] rises faster with the lower expression of Mdm2. When Mdm2 is deficient, HIF-$1\alpha_{ac}$ stays at high levels for a rather long period. This corresponds to the abnormal expression of HIF-1 in tumor cells due to the mutation of p53 [36].

3.6. p300 abundance affects the competition between HIF-1α and p53

Given HIF-1 and p53 compete for limited p300 [11], we further investigate how the total level of p300 influences their competition (Figure 8A and 8B). When the total level of p300, $p300_{tot}$, is reduced to 5 (half the standard value), the steady-state behaviors of [HIF-$1\alpha_{ac}$] and [$p53_{ac}$] change thoroughly in moderate and severe hypoxia (Figure 8A). Under moderate hypoxia, HIF-1α is activated to induce CSB to repress p53. Under severe hypoxia, the further reduction in p300 abundance leads to enhanced competition. HIF-$1\alpha_{ac}$ predominates over p53 in the competition for p300, further rising to high levels. By contrast, p53 cannot be fully activated and drops to low levels.

With excessive p300 ($p300_{tot}$ = 50), the inhibitory effect of HIF-1α on p53 becomes inapparent and [$p53_{ac}$] gradually accumulates from medium levels under mild hypoxia (Figure 8B). Due to sufficiency

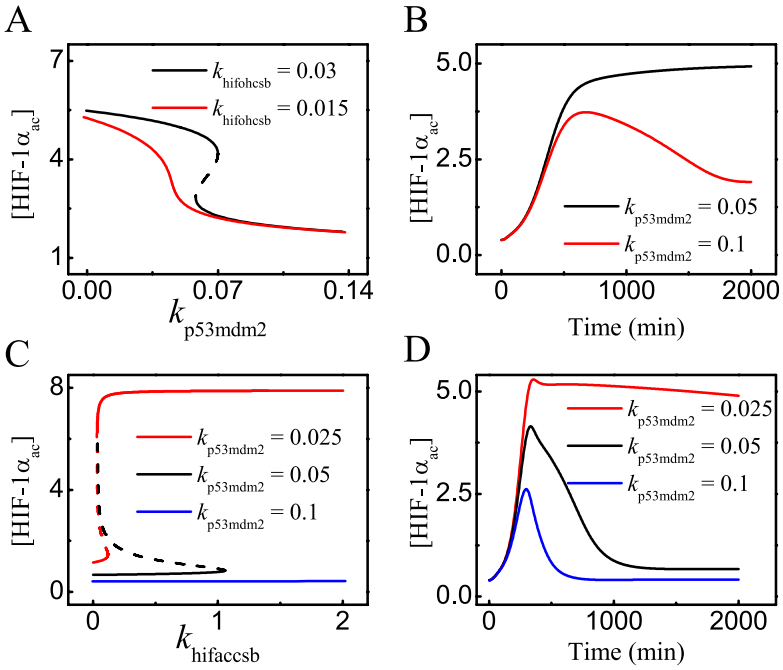

Figure 7. Antagonistic p53-Mdm2-HIF-1α and HIF-1α-CSB positive feedback loops. (A) The bifurcation diagrams of [HIF-1α_{ac}] versus $k_{p53mdm2}$ (the induction rate of Mdm2 by p53) at 0.4% O_2. (B) The dynamics of [HIF-1α_{ac}] at 0.4% O_2 with different $k_{p53mdm2}$. (C) The bifurcation diagram of [HIF-1α_{ac}] versus $k_{hifaccsb}$ at 0.02% O_2 with different $k_{p53mdm2}$. (D) The dynamics of [HIF-1α_{ac}] at 0.02% O_2 with different $k_{p53mdm2}$.

in p300 availability, both HIF-1α_{ac} and $p53_{ac}$ stays at fairly high levels under severe hypoxia. It seems that only when the amount of p300 is limited, the HIF-1α_{ac}-CSB positive feedback loop functions in the activation of HIF-1α. Taking the target genes into account, the abundance of p300 is critical to cell fate decision.

We plot the bifurcation diagrams of [HIF-1α_{ac}] versus p300-dependent acetylation rate of HIF-1α, $k_{hifp300}$, for different k_{csbp53} or $k_{p53p300}$ (Figure 8C and 8D). The steady-state level of HIF-1α_{ac} exhibits bistability with varying $k_{hifp300}$ under severe hypoxia. Similar to the case with standard parameter setting, [HIF-1α_{ac}] stays at low levels for $k_{hifp300}$ below the threshold since it loses the competition for p300. When $k_{hifp300}$ becomes rather large and exceeds the threshold, HIF-1α wins the competition even under severe hypoxia. Moreover, increasing k_{csbp53} reduces the threshold of $k_{hifp300}$ for HIF-1α activation since high expression of CSB promotes HIF-1α activation by repressing p53. On the contrary, increasing $k_{p53p300}$ counteracts the effects of increasing $k_{hifp300}$ on HIF-1α activation, thereby raising the threshold for HIF-1α activation (Figure 8D).

4. Discussion

This work investigated how HIF-1α and p53 compete for the predominance in response to hypoxia. The overall picture of the hypoxic response involving HIF-1α and p53 pathways is presented in a

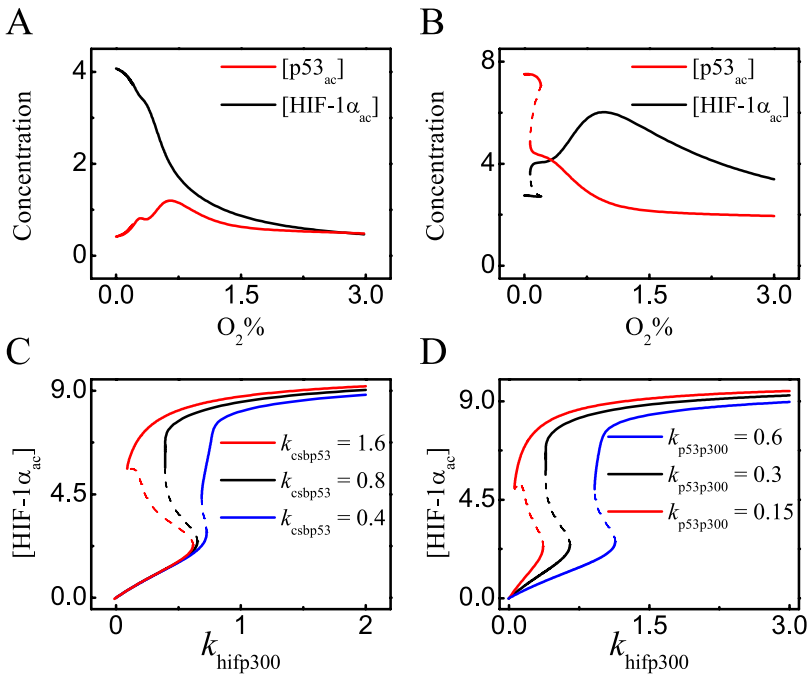

Figure 8. p300 abundance influences the competition between HIF-1α and p53. (A-B) Bifurcation diagrams of [HIF-1α_{ac}] and [p53$_{ac}$] versus O_2% with p300$_{tot}$ = 5 (A) or 50 (B). (C-D) Bifurcation diagrams of [HIF-1α_{ac}] versus $k_{hifp300}$ (p300-dependent acetylation rate of p53) for different k_{csbp53} (association rate of CSB and p53) (C) or $k_{p53p300}$ (binding rates of p300 and p53) (D) at 0.02% O_2.

schematic diagram (Figure 9). For mild hypoxia, PHD is deactivated and HIF-1α is stabilized and its N-TAD transcriptional activity is activated. p53 is undetected due to Mdm2-dependent degradation. For moderate hypoxia, the C-TAD activity of HIF-1 is further activated. p53 accumulates partially due to the ATR-independent mechanism. HIF-1α induces CSB to promote its own activation by inhibiting p53 activity. HIF-1α induces PFKL and VEGF to trigger glycolysis and angiogenesis, respectively. In severe hypoxia, p53 accumulates markedly and prevails over HIF-1α in the competition for p300. By degrading HIF-1α through modulating Mdm2, p53 guarantees the low level of HIF-1α under severe hypoxia, amplifying its own activation. As a result, activated p53 induces PUMA to initiate apoptosis. The coupled HIF-1α-CSB-p53, p53-Mdm2 and p53-Mdm2-HIF-1α feedback loops coordinate in regulating the two transcription factors under different hypoxic conditions. In addition, p300 abundance is a key factor modulating the interplay between HIF-1α and p53.

Modeling the cellular response to hypoxia has attracted intensive interests. Most studies by others focused on the mechanism for HIF-1α activation upon hypoxia [19]. Our present work focused on the modulation of the competition between HIF-1α and p53 by their target genes. Several feedback loops interplay to influence the competition and cell fate. Our work reveals the competition between HIF-1α and p53 through their target genes CSB and Mdm2.

There still exist some limitations in our model. It has been identified that FIH also influences the stability of HIF-1α in addition to its role in repressing HIF-1α activity [21]. The effect of FIH on

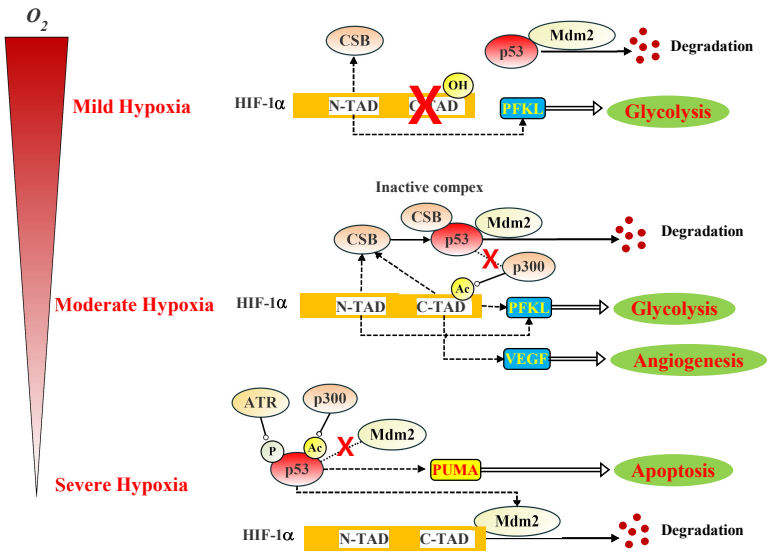

Figure 9. Schematic diagram of the competition between HIF-1 and p53 under different hypoxic conditions. Transactivation is denoted by arrow-headed dashed lines, while transition is represented by arrow-headed solid lines. Circle-headed lines denote promotion. Dotted lines represent interaction between proteins, while red crosses denote the inhibition of interaction or activity.

HIF-1α stability is ignored in the present model. We did not consider the N-TAD hydroxylated form of HIF-1α since it is dehydroxylated due to deactivation of PHD upon hypoxia [24]. The role of Mdm2 in the hypoxic response is rather complicated. It was reported that Mdm2 can stabilize HIF-1α in mild hypoxia in a p53-independent way [37]. It is a challenge to unravel how Mdm2 transits its role under different hypoxic conditions. Moreover, HIF-1α-induced CITED2 may affect the crosstalk between HIF-1 and p53 pathways by inhibiting p300-dependent HIF-1 activation [38, 39]. There is an antagonistic relationship between CITED2 and CSB, which may also interfere with p53 activation [40]. Thus, it is intriguing to construct a more detailed model of the hypoxic response.

Both the HIF-1 and p53 pathways play significant roles in cellular response to hypoxia. Our work proposed a new mechanism by which HIF-1 modulates the activation of p53 through its target gene CSB. For abnormally high expression of HIF-1 in tumor cells, it should be feasible to knock down CSB, killing the cells by enhancing apoptosis. Moreover, it would be promising to exploit Mdm2-dependent HIF-1α degradation in cancer therapy.

Acknowledgments

This work was supported by the National Natural Science Foundation of China (Nos. 11574139, 11547025 and 11874209) and the Fundamental Research Funds for the Central Universities (Nos. 14380013 and 14380015).

Conflict of interest

The authors declare there is no conflict of interest.

References

1. G. L. Semenza, Hypoxia-inducible factors in physiology and medicine, *Cell*, **148** (2012), 399–408.
2. C. J. Schofield and P. J. Ratcliffe, Oxygen sensing by HIF hydroxylases, *Nat. Rev. Mol. Cell Biol.*, **5** (2004), 343–354.
3. M. Ivan, K. Kondo, H. F. Yang, et al., HIF targeted for VHL-mediated destruction by proline hydroxylation: Implications for O_2 sensing, *Science*, **292** (2001), 464–468.
4. D. Lando, D. J. Peet, J. J. Gorman, et al., FIH-1 is an asparaginyl hydroxylase enzyme that regulates the transcriptional activity of hypoxia-inducible factor, *Genes Dev.*, **16** (2002), 1466–1471.
5. F. Dayan, D. Roux, M. C. Brahimi-Horn, et al., The oxygen sensor factor-inhibiting hypoxia-inducible factor-1 controls expression of distinct genes through the bifunctional transcriptional character of hypoxia-inducible factor-alpha, *Cancer Res.*, **66** (2006), 3688–3698.
6. K. T. Bieging, S. S. Mello and L. D. Attardi, Unravelling mechanisms of p53-mediated tumour suppression, *Nat. Rev. Cancer*, **14** (2014), 359–370.
7. X.-P. Zhang, F. Liu, Z. Cheng, et al., Cell fate decision mediated by p53 pulses, *Proc. Natl. Acad. Sci. USA*, **106** (2009), 12245–12250.
8. X.-P. Zhang, F. Liu and W. Wang, Two-phase dynamics of p53 in the DNA damage response, *Proc. Natl. Acad. Sci. USA*, **108** (2011), 8990–8995.
9. C. H. Zhou, X. P. Zhang, F. Liu, et al., Modeling the interplay between the HIF-1 and p53 pathways in hypoxia, *Sci. Rep.*, **5** (2015), 13834.
10. S. Filippi, P. Latini, M. Frontini, et al., CSB protein is (a direct target of HIF-1 and) a critical mediator of the hypoxic response, *EMBO J.*, **27** (2008), 2545–2556.
11. T. Schmid, J. Zhou, R. Kohl, et al., p300 relieves p53-evoked transcriptional repression of hypoxia-inducible factor-1 (HIF-1), *Biochem. J.*, **380** (2004), 289–295.
12. M. Frontini and L. Proietti-De-Santis, Cockayne syndrome B protein (CSB) linking p53, HIF-1 and p300 to robustness, lifespan, cancer and cell fate decisions, *Cell Cycle*, **8** (2009), 693–696.
13. R. V*é*lez-Cruz and J. M. Egly, Cockayne syndrome group B (CSB) protein: At the crossroads of transcriptional networks, *Mech. Ageing Dev.*, **134** (2013), 234–242.
14. W. G. An, M. Kanekal, M. C. Simon, et al., Stabilization of wild-type p53 by hypoxia-inducible factor 1α, *Nature*, **392** (1998), 405–408.
15. D. Chen, M. Li, J. Luo, et al., Direct interactions between HIF-1α and Mdm2 modulate p53 function, *J. Biol. Chem.*, **278** (2003), 13595–13598.
16. E. M. Hammond, N. C. Denko, M. J. Dorie, et al., Hypoxia links ATR and p53 through replication arrest, *Mol. Cell Biol.*, **22** (2002), 1834–1843.

17. A. Sermeus and C. Michiels, Reciprocal influence of the p53 and the hypoxic pathways, *Cell Death Dis.*, **2** (2011), e164.

18. J. S. Fridman and S. W. Lowe, Control of apoptosis by p53, *Oncogene*, **22** (2003), 9030–9040.

19. Z. Fábián, C. T. Taylor and L. K. Nguyen, Understanding complexity in the HIF signaling pathway using systems biology and mathematical modeling, *J. Mol. Med.*, **94** (2016), 377–390.

20. A. A. Qutub and A. S. Popel, A computational model of intracellular oxygen sensing by hypoxia-inducible factor HIF1α, *J. Cell Sci.*, **119** (2006), 3467–3480.

21. L. K. Nguyen, M. A. S. Cavadas, C. C. Scholz, et al., A dynamic model of the hypoxia-inducible factor 1α (HIF-1α) network, *J. Cell Sci.*, **126** (2013), 1454–1463.

22. J. Bagnall, J. Leedale, S. E. Taylor, et al., Tight control of hypoxia-inducible factor-α transient dynamics is essential for cell survival in hypoxia, *J. Biol. Chem.*, **289** (2014), 5549–5564.

23. P. Koivunen, M. Hirsilä, V. Günzler, et al., Catalytic properties of the asparaginyl hydroxylase (FIH) in the oxygen sensing pathway are distinct from those of its prolyl 4-hydroxylases, *J. Biol. Chem.*, **279** (2004), 9899–9904.

24. Y. Tian, K. K. Yeoh, M. K. Lee, et al., Differential sensitivity of HIF hydroxylation sites to hypoxia and hydroxylase inhibitors, *J. Biol. Chem.*, **286** (2011), 13041–13051.

25. R. Ravi, B. Mookerjee, Z. M. Bhujwalla, et al., Regulation of tumor angiogenesis by p53-induced ubiquitin-mediated degradation of hypoxia-inducible factor-1α, *Genes Dev.*, **14** (2000), 34–44.

26. S. J. Lee, C. J. Lim, J. K. Min, et al., Protein phosphatase 1 nuclear targeting subunit is a hypoxia inducible gene: its role in post-translational modification of p53 and MDM2, *Cell Death. Differ.*, **14** (2007), 1106–1116.

27. G. L. Semenza, P. H. Roth, H. M. Fang, et al., Transcriptional regulation of genes encoding glycolytic-enzymes by hypoxia-inducible factor-1, *J. Biol. Chem.*, **269** (1994), 23757–23763.

28. J. A. Forsythe, B. H. Jiang, N. V. Iyer, et al., Activation of vascular endothelial growth factor gene transcription by hypoxia-inducible factor 1, *Mol. Cell Biol.*, **16** (1996), 4604–4613.

29. S. Z. Liu, B. Shiotani, M. Lahiri, et al., ATR autophosphorylation as a molecular switch for checkpoint activation, *Mol. Cell*, **43** (2011), 192–202.

30. B. D. Manning and L. C. Cantley, AKT/PKB signaling: Navigating downstream, *Cell*, **129** (2007), 1261–1274.

31. A. J. Levine and M. Oren, The first 30 years of p53: growing ever more complex, *Nat. Rev. Cancer*, **9** (2009), 749–758.

32. Y. Yu, G. Wang, R. Simha, et al., Pathway switching explains the sharp response characteristic of hypoxia response network, *PLoS Comput. Biol.*, **3** (2007), e171.

33. R. L. Weinberg, D. B. Veprintsev, M. Bycroft, et al., Comparative binding of p53 to its promoter and DNA recognition elements, *J. Mol. Biol.*, **348** (2005), 589–596.

34. M. Y. Koh and G. Powis, Passing the baton: the HIF switch, *Trends Biochem. Sci.*, **37** (2012), 364–372.

35. M. Caputo, M. Frontini, R. Velez-Cruz, et al., The CSB repair factor is overexpressed in cancer cells, increases apoptotic resistance, and promotes tumor growth, *DNA Rep.*, **12** (2013), 293–299.

36. J. A. Bertout, S. A. Patel and M. C. Simon, The impact of O_2 availability on human cancer, *Nat. Rev. Cancer*, **8** (2008), 967–975.

37. Y. M. Lee, J. H. Lim, Y. S. Chun, et al., Nutlin-3, an Hdm2 antagonist, inhibits tumor adaptation to hypoxia by stimulating the FIH-mediated inactivation of HIF-1α, *Carcinogenesis*, **30** (2009), 1768–1775.

38. S. Bhattacharya, C. L. Michels, M. K. Leung, et al., Functional role of p35srj, a novel p300/CBP binding protein, during transactivation by HIF-1, *Genes Dev.*, **13** (1999), 64–75.

39. D. H. Shin, S. H. Li, Y. S. Chun, et al., CITED2 mediates the paradoxical responses of HIF-1α to proteasome inhibition, *Oncogene*, **27** (2008), 1939–1944.

40. K. Mattes, G. Berger, M. Geugien, et al., CITED2 affects leukemic cell survival by interfering with p53 activation, *Cell Death Dis.*, **8** (2017), e3132.

AIMS Press